Finite size induces crossover temperature in growing spin chains

Julian Sienkiewicz, Krzysztof Suchecki, and Janusz A. Hołyst
Faculty of Physics, Center of Excellence for Complex Systems Research, Warsaw University of Technology, Koszykowa 75, PL-00-662 Warsaw, Poland

(Received 3 July 2013; revised manuscript received 12 December 2013; published 7 January 2014)

We introduce a growing one-dimensional quenched spin model that bases on asymmetrical one-side Ising interactions in the presence of external field. Numerical simulations and analytical calculations based on Markov chain theory show that when the external field is smaller than the exchange coupling constant J there is a nonmonotonous dependence of the mean magnetization on the temperature in a finite system. The crossover temperature T_c corresponding to the maximal magnetization decays with system size, approximately as the inverse of the Lambert W function. The observed phenomenon can be understood as an interplay between the thermal fluctuations and the presence of the first cluster determined by initial conditions. The effect exists also when spins are not quenched but fully thermalized after the attachment to the chain. By performing tests on real data we conceive the model is in part suitable for a qualitative description of online emotional discussions arranged in a chronological order, where a spin in every node conveys emotional valence of a subsequent post.

DOI: 10.1103/PhysRevE.89.012105 PACS number(s): 02.50.Ga, 75.10.Pq, 05.50.+q, 87.23.Ge

I. INTRODUCTION

Due to their simplicity and fully analytical treatment, one-dimensional models are useful and comprehensible objects for theoretical studies. Of the exceptional importance backed by the feasibility of calculations is the Ising model [1–12]. Such a system with short-range ferromagnetic interactions possesses no crossover temperature when system's susceptibility is observed. This is true for a nongrowing system and when each spin is symmetrically coupled to its left and right neighbor [13]. In this paper we introduce an evolving spin model with an asymmetrical one-side dynamics. However, the asymmetry is unlike the one proposed by Huang [14,15], where the spin variable can take on two eigenvalues $+1$ and $-1/\lambda$ with $\lambda > 1$, nor is it connected to the degeneration of higher-energy spin state [16]. Instead, we explicitly modify the Ising Hamiltonian by taking into account only node's left neighbor as well as equip our model with a growing component (a new node is quenched after a single update). We show that under nonzero external field smaller than interaction constant, the model exhibits a *crossover temperature* where the mean magnetization is maximal. This phenomenon is further explained as an interplay between the thermal fluctuations and the first spin cluster determined by initial conditions.

Although one-dimensional systems are frequently used to model social dynamics [17–21], such an approach often suffers from over-simplicity, e.g., one finds no evidence to support the idea that agents related to social interactions are to be distributed on a chain. In this paper we give clear reasons for choosing this very topology. In fact, our model is motivated by the recent research [22,23] on affective interactions among participants of Internet fora [24–26]. Such media often use a chronological structure of the incoming posts that can be easily regarded as a one-dimensional chain (i.e., the consecutive posts are represented by the nodes in the chain). The results of our previous analyses [22,23] indicate that one of the most dominant phenomena seen in such media is a strong dependence of the expressed emotion on the emotion of the last comment (i.e., the newest one).

II. MODEL DESCRIPTION

The model bases on the idea of a growing chain (see Fig. 1). The process is organized as follows: the first node of the chain has a random spin $s_0 = \pm 1$ (that could be interpreted as emotional valence [27] of a post in online discussion), that is drawn with probability $\Pr(s_0 = \pm 1) = 1/2$ [Figs. 1(a)–1(b)]. Then, another node of the chain is added to the right side of the last one [Fig. 1(c)] and it is initially equipped with a spin once again drawn with equal probabilities $\Pr(s_1 = \pm 1) = 1/2$. Subsequently, the node becomes a subject to the updating procedure that is based on the Ising-like model approach [Fig. 1(d)]. For each new node n, we define a function $\mathcal{E}_n = -Js_{n-1}s_n - hs_n$, where the constant $J > 0$ corresponds to exchange integral in the Ising model and h is the external field. A minimum of the function $\mathcal{E}_n$ conforms to spins of the same sign in the consecutive nodes of the chain, thus $\mathcal{E}_n$ can be treated as an *emotional discomfort* function felt by a user posting a message s_n. As the spin is drawn, we test how flipping its sign to the opposite one (i.e., from $s_n = +1$ to $s_n = -1$ or likewise) affects the change of function $\mathcal{E}$ as $\Delta\mathcal{E} = \mathcal{E}'_n - \mathcal{E}_n = -(Js_{n-1} + h)(s'_n - s_n)$, where term $\mathcal{E}'_n$ corresponds to s'_n calculated when $s_n \to s'_n = -s_n$. Then we follow the Metropolis algorithm [28], i.e., if the $\Delta\mathcal{E} < 0$ we accept the change; otherwise, we test if the

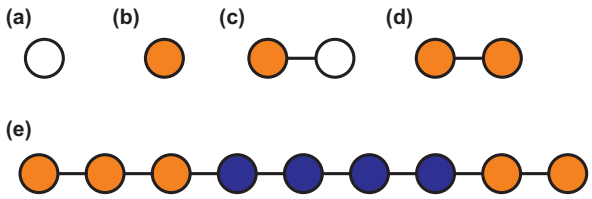

FIG. 1. (Color online) A scheme of the simulation process. (a)–(d) Consecutive steps of an exemplary simulation: (a) starting from an empty node, (b) adding random spin to the first node, (c) adding the next node, (d) inserting spin according to dynamics rule. (e) An effect of the simulation. Orange ($s = +1$) and blue ($s = -1$) discs symbolize spins.

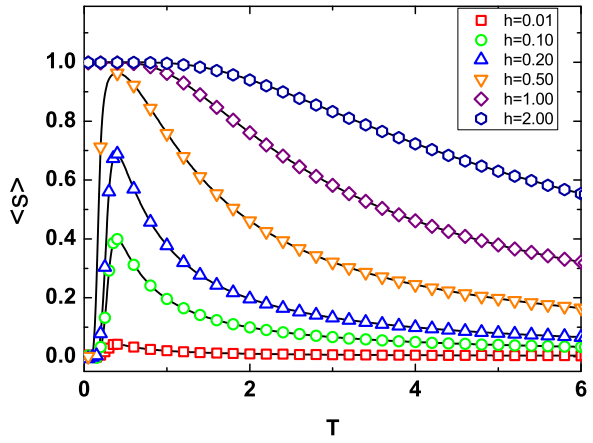

FIG. 2. (Color online) Average spin $\langle s\rangle$ as function of temperature T for different values of the external magnetic field (symbols). Solid lines come from Eqs. (4) and (5). All data points are for $N = 10^3$.

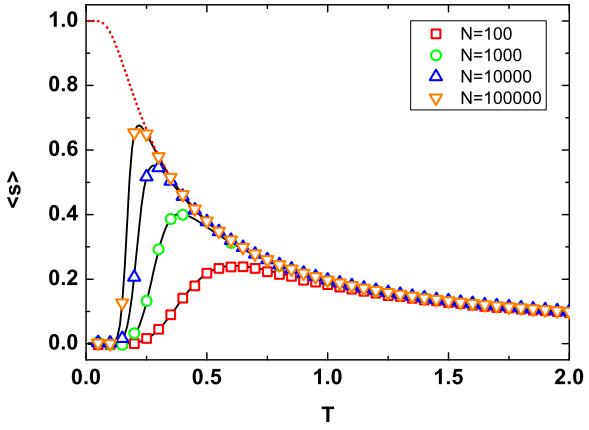

FIG. 3. (Color online) Average spin $\langle s\rangle$ as function of temperature T for different values of the chain size N (symbols); all data points for $h = 0.1$. Solid lines come from Eq. (4) and the dotted line is $\tanh(2h/T)$.

expression $\exp[-\Delta\mathcal{E}(k_BT)^{-1}]$ is smaller or larger than a random value $\xi \in [0;1]$ (here, k_B is Boltzmann constant and T is temperature). If the latter occurs, we accept the change; otherwise, the spin is kept as originally chosen. The procedure of adding new nodes and setting their spin variables according to the above-described rules is repeated until the size N of the chain is reached [Fig. 1(e)].

III. NUMERICAL SIMULATIONS

Without losing the generality all numerical simulations have been performed for $J = k_B = 1$. The average spin in the chain (an equivalent of the average emotion in online discussion) is calculated as $\langle s\rangle = \frac{1}{N}\sum_{n=1}^{N} s_n$ and afterwards averaged over M realizations (typically, in this study $M = 10^5$). Figure 2 shows the average spin $\langle s\rangle$ as a function of the temperature T for selected values of external field h. In the case of $h < 1$ the plot reveals $\langle s\rangle$ equal to zero for small $T \ll 1$, then a clear maximum for some specific crossover value T_c appears. Finally, a decrease toward zero for $T > T_c$ takes place. In the case of $h \geqslant 1$ such a phenomenon is not observed: instead, $\langle s\rangle = 1$ for small T and then there is a monotonous decrease toward zero.

Figure 3 shows that for smaller systems (e.g., $N = 10^2$) the crossover temperature T_c is of order 0.5–1 and is shifted toward lower values for larger systems. It is also interesting to track the dependence of the average spin value on the external field (see Fig. 4). In the case of low temperatures ($T < T_c$) average spin value changes abruptly from $\langle s\rangle = -1$ to $\langle s\rangle = 0$ for $h = -1$ and then from $\langle s\rangle = 0$ to $\langle s\rangle = 1$ for $h = 1$. For higher temperatures ($T > T_c$) this change is smoother and length range of h for which $\langle s\rangle \approx 0$ is smaller.

IV. ANALYTICAL DESCRIPTION

The system dynamics can be easily described using a two-state Markov chain approach [29]. The growth of the chain follows the transition matrix $\mathbf{P}$,

$$\mathbf{P} = \begin{bmatrix} p & 1-p \\ 1-q & q \end{bmatrix}, \tag{1}$$

with conditional probabilities $p = \Pr(+|+)$ and $q = \Pr(-|-)$. Matrix $\mathbf{P}$ defines probabilities evolution of both states $\Pr(s_n = \pm 1)$ as $\mathbf{s}_{n+1} = \mathbf{s}_n\mathbf{P}$, where $\mathbf{s}_n = [\Pr(s_n = +1) \quad \Pr(s_n = -1)]$. The average spin in the nth node is $\langle s_n\rangle = \mathbf{s}_0\mathbf{P}^n[1 \quad -1]^T$, with $\mathbf{s}_0 = [1/2 \quad 1/2]$. Finally, the mean $\langle s_n\rangle$ calculated over all nodes in the chain equals to

$$\langle s\rangle = \frac{p-q}{2-p-q}\left[1 + \frac{1}{N} - \frac{1-(p+q-1)^{N+1}}{N(2-p-q)}\right]. \tag{2}$$

The specific values of p and q for our model are

$$\begin{cases} p = \Pr(+|+) = 1 - \frac{1}{2}e^{-\widetilde{\beta}(h+J)} \\ q = \Pr(-|-) = \frac{1}{2} \pm \frac{1}{2} \mp \frac{1}{2}e^{\pm\widetilde{\beta}(h-J)} \end{cases}, \tag{3}$$

where upper signs correspond to case $|h| < J$, lower signs to $|h| \geqslant J$, and $\widetilde{\beta} = 2/(k_BT)$ (see the appendix for details). In further discussion we assume that $h > 0$, although all derivations and effects are also true for $h < 0$ with reversed spins. Different form of q for small and large $|h|$ follows from the interchange of energy level positions corresponding to states $s_n = s_{n+1} = -1$ and $s_n = -1, s_{n+1} = +1$ (see Fig. 6 and the appendix). Putting Eq. (3) into Eq. (2) we get the average spin in the chain for low magnetic fields $|h| < J$ as

$$\langle s\rangle_s = \tanh\widetilde{\beta}h\left[1 + \frac{1}{N} - \frac{1-(1-e^{-\widetilde{\beta}J}\cosh\widetilde{\beta}h)^{N+1}}{Ne^{-\widetilde{\beta}J}\cosh\widetilde{\beta}h}\right], \tag{4}$$

and for $|h| \geqslant J$ as

$$\langle s\rangle_l = \operatorname{sgn}(h)\frac{\cosh\widetilde{\beta}J - e^{\widetilde{\beta}|h|}}{\sinh\widetilde{\beta}J - e^{\widetilde{\beta}|h|}} \times\left[1 + \frac{1}{N} - \frac{1-(e^{-\widetilde{\beta}|h|}\sinh\widetilde{\beta}J)^{N+1}}{N(1-e^{-\widetilde{\beta}|h|}\sinh\widetilde{\beta}J)}\right]. \tag{5}$$

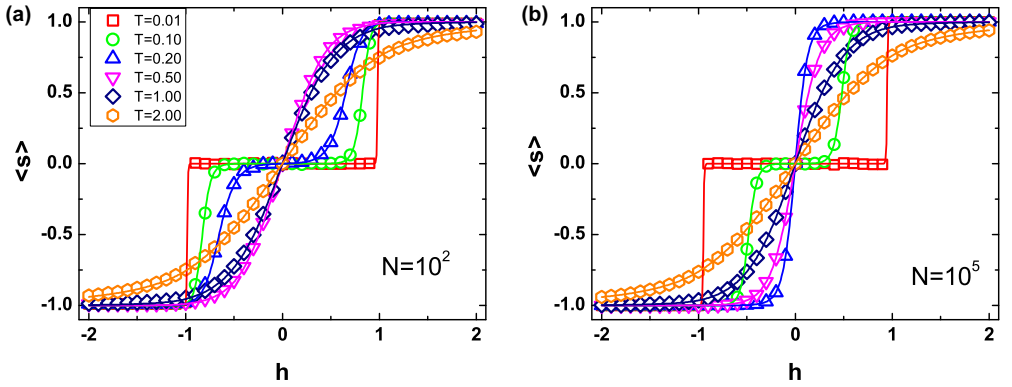

FIG. 4. (Color online) Average spin $\langle s \rangle$ as function of the external field h for different values of temperature T (symbols). Solid lines come from Eq. (4).

Let us note that factors standing in front of square brackets of Eqs. (4) and (5) describe the thermodynamical limit and coincide with the corresponding factor in Eq. (2). These analytical results are fully supported by numerical simulations (solid lines in Figs. 2, 3, and 4).

Both numerical and analytical approaches indicate crucial role played by the system's size N (see Fig. 5): for a constant value of external field h increasing N leads to a shift in T_c toward $T = 0$ as well as to an increase of the maximum value $\langle s \rangle(T_c)$. To get an analytical estimation of T_c we assume that $\widetilde{\beta} h \ll 1$, which gives the opportunity to rewrite Eq. (4) as

$$\langle s \rangle_s \approx \widetilde{\beta} h \left[1 + \frac{1}{N} - \frac{1 - (1 - e^{-\widetilde{\beta} J})^{N+1}}{N e^{-\widetilde{\beta} J}} \right]. \qquad (6)$$

Because it is linearly dependent on h, the factor is an equivalent of the susceptibility $(\frac{\partial \langle s \rangle_s}{\partial h})_{h=0}$ times h. If we further assume $N \gg 1$, and solve $\frac{\partial \langle s \rangle_s}{\partial T} = 0$, one can approximate T_c as

$$T_c \approx \frac{2J}{k_B \left[W(Ne) - 1 \right]}, \qquad (7)$$

where $W(...)$ is Lambert W function. Comparison between this approximation and numerical solution of Eq. (4) is shown in Fig. 5, providing evidence of good agreement for small values of h as expected.

V. PHENOMENOLOGICAL DESCRIPTION

The striking difference between average spin values for low and high fields h—as presented by Eqs. (4) and (5)—can be explained as follows. For $0 < h < J$ [Fig. 6(a)] the four states system of two last spins s_{n-1} and s_n possess two lowest-energy states corresponding to parallel ordering of both spins $s_{n-1} = s_n = -1$ and $s_{n-1} = s_n = +1$. Such a system is *bistable* and temperature causes a random switching between clusters (domains) of opposite spin values. The average length

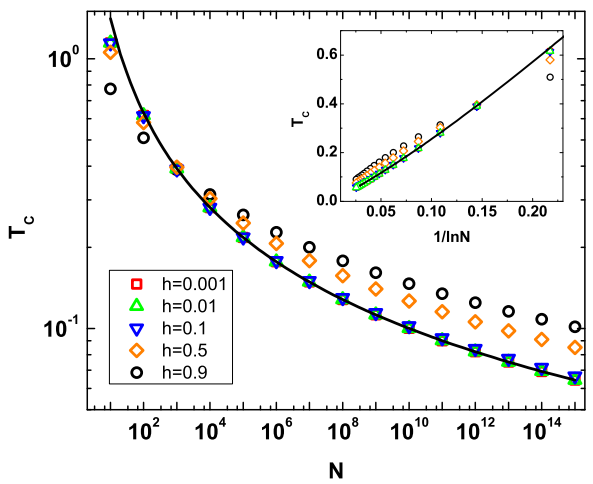

FIG. 5. (Color online) Crossover temperature T_c versus the size of the chain N. Symbols are numerical solution of Eq. (4) while the solid line comes from Eq. (7). Note that decay of T_c is very slow. The symbols for three lowest h values overlap. The inset shows T_c versus $1/\ln N$.

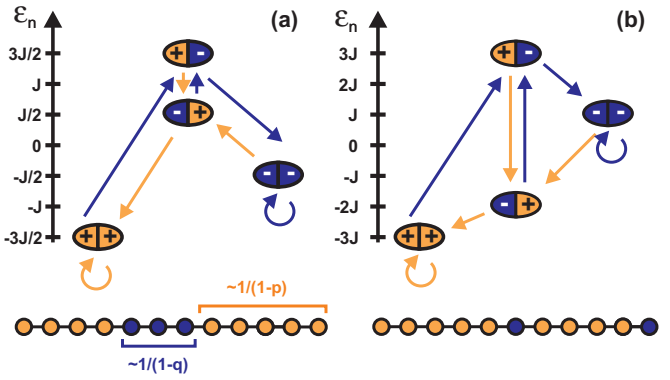

FIG. 6. (Color online) Possible states of the *last two* spins of the chain (the last is on the right of the pair) and the associated energies $\mathcal{E}_n$ tied to the last spin n. Arrows show how adding new + (orange) or − (blue) spin changes last two spin state (they are not the same spins after such step). Note that energy of starting state is of no importance, only relation between levels of possible destinations. The first situation ($0 < h = J/2 < J$) is bistable with two energy minima corresponding to states $s_{n-1} = s_n = +1$ and $s_{n-1} = s_n = -1$, while second $h = 2 > J$ is monostable.

l_+ of a spin-up cluster is $l_+ = 1/(1-p)$, while corresponding length l_- of spin-down cluster is $l_- = 1/(1-q)$. Note that in the thermodynamical limit Eq. (2) can be written as $\langle s\rangle = (\frac{l_+}{l_-} - 1)/(\frac{l_+}{l_-} + 1)$. The quotient l_+/l_- for $|h| < J$ is equal to $e^{2\widetilde{\beta}h}$, thus it is independent from J. Of course, with increasing J lengths l_+, l_- of both types of clusters increase but it does not influence the mean spin $\langle s\rangle$ of the *infinite* chain. After crossing the critical value of the magnetic field $h = J > 0$ the situation changes. The energy $\mathcal{E}_n$ for $s_{n-1} = s_n = -1$ is higher than the energy $\mathcal{E}_n$ for $s_{n-1} = -1$, $s_n = +1$, making system *monostable*—thus the temperature mostly causes *single* spins $s_n = -1$ to appear in the chain dominated by the stable $s_n = +1$ phase. It means that there are no clusters of negative spins [Fig. 6(b)] for $|h| > J$ and the mean magnetization depends mainly on the density of single-spin impurities. In fact, for $h = J$ we have $l_- = 2$ and l_- further decays with the increase of h. However, the density of single-spin impurities is a decreasing function of an energy of interface between $s_{n-1} = +1$ and $s_n = -1$ that is dependent on the coupling constant J. This leads to a profound difference between mean values of spins in the chain in the case of the thermodynamical limit of Eqs. (4) and (5). The first one takes the form of $\langle s\rangle_s = \tanh\widetilde{\beta}h$, which is independent of J. In fact, for a chain of a finite length N there is always an influence of the boundary condition that leads to the emergence of the first (boundary) cluster with spins up or spins down. Due to the assumed symmetry $\Pr(s_0 = \pm 1) = 1/2$, both types of these boundary clusters are represented with the same probability. It follows that a short chain possesses a zero-mean magnetization when one averages it over an ensemble of initial and boundary conditions, which can be observed in Fig. 3. While increasing the length N, the chain magnetization depends more and more on the ratio between lengths l_+/l_- of positive and negative clusters. It follows that the effect of the boundary condition disappears the faster and the smaller is the coupling constant J responsible for spin clustering. In the thermodynamical limit the presence of the boundary cluster can be disregarded and the magnetization does not depend on the coupling J. This phenomenological picture can also justify a nonmonotonous dependence of mean magnetization on the temperature when $|h| < J$. When the temperature is low, the length of initial cluster tends to infinity, thus mean magnetization can be close to zero even for large systems because of a random, symmetric initial condition. If the temperature increases both lengths l_+,l_- decay, and thus the effect of boundary conditions becomes less important and the mean magnetization increases toward magnetization of infinite chain governed by l_+/l_-. However, the ratio l_+/l_- decreases with T, thus for higher temperatures $\langle s\rangle$ decreases toward 0. It follows there is a *crossover temperature* T_c where the magnetization is maximal in the effect of interplay between the initial condition and temperature fluctuations (see Fig. 3). This crossover temperature decays with system size N (see Fig. 5), since for larger systems the impact of the first cluster is very small. Let us note that for $|h| > J$, when no clusters are present in the system there is no crossover temperature and the magnetization in the thermodynamical limit depends on the coupling constant J: $\langle s\rangle_l \approx \mathrm{sgn}(h)(\cosh\widetilde{\beta}J - e^{\widetilde{\beta}|h|})/(\sinh\widetilde{\beta}J - e^{\widetilde{\beta}|h|})$.

VI. COMPARISON WITH CLASSICAL 1D ISING MODEL

It is of use to compare and contrast the obtained results with the classical one-dimensional Ising model (e.g., Ref. [13]). The most noticeable difference undoubtedly regards the foundations of the model—in the classical case the length of the chain is fixed and each node n is initially filled with a spin $s_n = \pm 1$. All spins can repeatedly change in time and their dynamics involve energy coupling with both neighbors. In our model, the chain grows, and only the newest spin added is subject to dynamics for a single time step, taking only its predecessor into account, after which it is quenched and unchanging. This equates the system size N to time t. This equivalence is the main reason for the existence of the crossover temperature in our model—investigating a chain of *finite length* is therefore the same as observing a system after a *finite time*. In fact, if we observe a classical Ising chain after a finite time, it is also possible to detect the crossover temperature. To show it, let us consider a normal Ising model, with a chain of length N and a normal spin dynamics, where the spins change in each step according to interactions with both their neighbors and an external field $|h| < J$. We will observe the mean spin $\langle s\rangle$ of the chain during a finite time t. Since the effect appears due to boundary conditions, the detailed condition affects the results.

We shall study two different boundary conditions that could mimic the random $+1$ or -1 spin in our model: (a) a chain initially fully ordered with equally probable $+1$ and -1 state, and (b) a chain with one spin pinned as $+1$ or -1 throughout the dynamics. In the first case, we consider the dynamics across *time*, thus we look at different dynamics time t, while in the second we consider dynamics across *space*, looking at different chain lengths N. As seen in Figs. 7(a) and 7(b) (the letter corresponds to the type of boundary conditions), the behavior of $\langle s\rangle$ versus T is different in those two approaches—in the first case it is similar to our growing chain model. This is because the one-directional nature of the interactions, explicit in our growing chain model, and implied by causality in the normal Ising chain over time, is crucial for the appearance of the crossover temperature. In the first case, the one-directional interactions mean that the initial condition creates an ordered cluster of limited size. In the second case, the cluster does not form, because following spins interfere with the process—a spin is very unlikely to order opposite to both external field and following spin. In fact, even if such a cluster does emerge at random, it will quickly shrink. This means that the size of our growing chain model behaves more like time than chain length in normal Ising model. The difference in behavior, decided by one- or two-directionality of interactions, can be also explained by how the system size N influences the properties of the system. As shown below, the one-directional interactions lead to a slow relaxation toward system equilibrium, which allows for an observation of crossover temperature at a finite time, while two-directional interactions lead to a very fast convergence to limit behavior. The fast convergence for two-directional interactions means that only very short chains can display any effects related to boundary condition (as seen in Fig. 7).

The magnetization per spin for $J > 0$ (ferromagnetic case)—an equivalent of $\langle s\rangle$ in the case of the classical

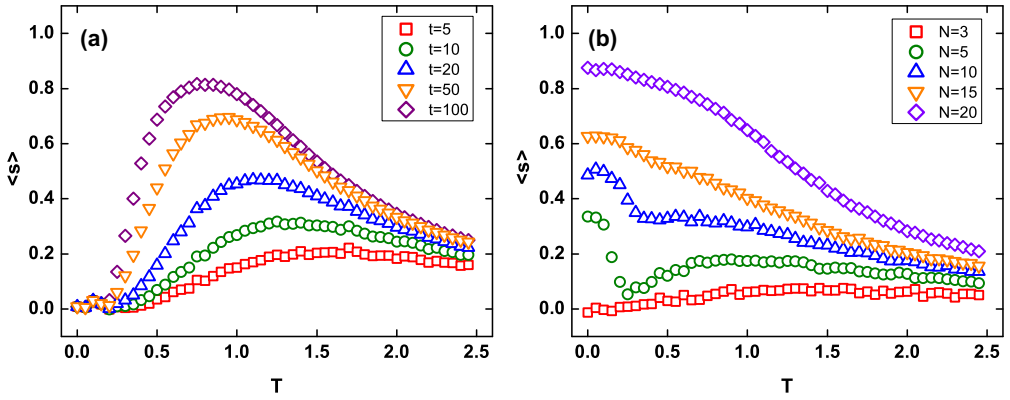

FIG. 7. (Color online) The mean spin $\langle s \rangle$ vs temperature T in the normal Ising model, when: (a) the chain is initially ordered and observed over different times t with $N = 20$, (b) the chain has one pinned spin and is observed for different lengths N for $t = 100$. In both cases the external field $h = 0.3$ is smaller than interaction strength $J = 1$ and the results are averaged over 10 000 realizations. The behavior for the case (a) is very similar to the one observed for our growing chain model (Fig. 3).

one-dimensional Ising model—is given by

$$m(h,T,N) = \frac{\sinh \beta h}{\sqrt{\sinh^2 \beta h + e^{-4\beta J}}} \frac{1 - \left(\frac{\lambda_-}{\lambda_+}\right)^N}{1 + \left(\frac{\lambda_-}{\lambda_+}\right)^N}, \tag{8}$$

where

$$\lambda_\pm = e^{\frac{1}{T}} (\cosh \beta h \pm \sqrt{e^{-4\beta J} + \sinh^2 \beta h}) \tag{9}$$

are the eigenvalues of the transfer matrix [13]. The magnetization is a strictly monotonous decaying function of T starting from $m = 1$ for $h > 0$ and it rapidly converges with system size N to its asymptotic value. On the other hand, from Eq. (7) it can be concluded that for our model, this convergence is much slower. The dependence of T_c is even slower, as $1/\ln N$ [see Eq. (7) and Fig. 5]. A comparison of the influence of the chain size in both models is presented in Fig. 8,

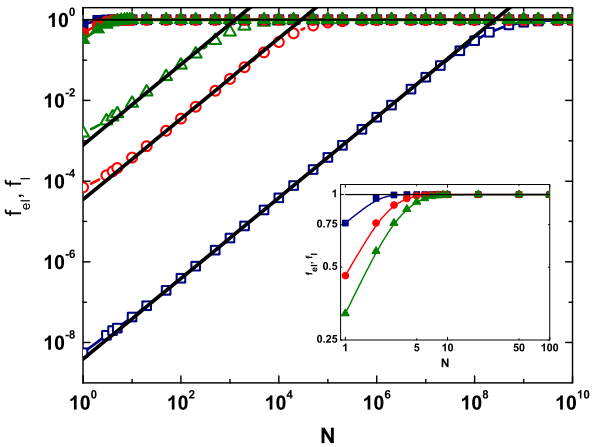

FIG. 8. (Color online) Factors f (for our model, empty symbols) and f_I (for the classical Ising model, filled symbols) versus the size of the chain N for $h = 0.1$. Symbols (squares for $T = 0.1$, circles $T = 0.2$, triangles for $T = 0.3$) come from Eqs. (10) and (11), while straight lines are from Eq. (12). The inset magnifies the results for the Ising model for $N \in [1; 100]$.

where

$$f = 1 + \frac{1}{N} - \frac{1 - (1 - e^{-\widetilde{\beta} J} \cosh \widetilde{\beta} h)^{N+1}}{N e^{-\widetilde{\beta} J} \cosh \widetilde{\beta} h} \tag{10}$$

and

$$f_I = \frac{1 - \left(\frac{\lambda_-}{\lambda_+}\right)^N}{1 + \left(\frac{\lambda_-}{\lambda_+}\right)^N} \tag{11}$$

are the factors in, respectively, $\langle s \rangle_s$ [see Eq. (4)] and $m(h,T,N)$ [see Eq. (8)], that are dependent on the chain size N. Factor f_I quickly converges to 1, e.g., for $J = k_B = 1$, $h = 0.1$ and $T = 0.1$ one needs as little as $N_c = 10$ to have $|f_I(N \to \infty) - f_I(N_c)| < 0.001$, while the factor f, depending on the value of T and h, can need a large chain length in order to reach the thermodynamic limit. In fact, for small T, Eq. (10) can be approximated by

$$f \approx \tfrac{1}{2}(N+1) e^{-\widetilde{\beta} J} \cosh \widetilde{\beta} h, \tag{12}$$

shown as straight lines in Fig. 8, which in turn can be used to estimate the critical value of N for which f is equal to one as $N_c \approx 4 e^{\widetilde{\beta}(J-h)}$. Thus, for $J = k_B = 1$, $T = 0.1$, and $h = 0.1$, we get $N_c \approx 2.6 \times 10^8$.

VII. COMPLETE THERMALIZATION OF INDIVIDUAL SPINS

If instead of performing a single Metropolis update of the newly attached spin we allow it to fully thermalize, then our newly added spin n is essentially drawn from the canonical ensemble. Therefore, the probabilities p and q can be derived by using Boltzmann factors.

The probability $p = \Pr(+|+)$ is

$$p = \frac{e^{-\beta \mathcal{E}_n(+1)}}{e^{-\beta \mathcal{E}_n(+1)} + e^{-\beta \mathcal{E}_n(-1)}}, \tag{13}$$

where $\mathcal{E}_n(s_n) = -Js_{n-1}s_n - hs_n$. If we put it into our formula, we obtain

$$p = \Pr(+|+) = \frac{e^{\beta(J+h)}}{e^{\beta(J+h)} + e^{-\beta(J+h)}}, \tag{14}$$

which further implies that

$$1 - p = \Pr(-|+) = \frac{e^{-\beta(J+h)}}{e^{\beta(J+h)} + e^{-\beta(J+h)}}. \tag{15}$$

Similarly, the probabilities q and $1 - q$ can be written as

$$q = \Pr(-|-) = \frac{e^{\beta(J-h)}}{e^{\beta(J-h)} + e^{-\beta(J-h)}}, \tag{16}$$

$$1 - q = \Pr(+|-) = \frac{e^{-\beta(J-h)}}{e^{\beta(J-h)} + e^{-\beta(J-h)}}. \tag{17}$$

Using the Markov chain approach [Eq. (2)], we can determine the mean spin $\langle s \rangle$ and finally write it as

$$\langle s \rangle = \frac{\sinh \widetilde{\beta} h}{\cosh \widetilde{\beta} h + e^{-\widetilde{\beta} J}} \left[1 + \frac{1}{N} - \frac{1 - u^{N+1}}{N(1-u)} \right], \tag{18}$$

where

$$u = \frac{\sinh \widetilde{\beta} J}{2 \cosh \frac{\widetilde{\beta}(h+J)}{2} \cosh \frac{\widetilde{\beta}(h-J)}{2}}. \tag{19}$$

The behavior of the model with spin thermalization, while somewhat different quantitatively from the single-update approach, is still qualitatively the same, exhibiting the maximum of $\langle s \rangle(T)$. One notable difference is the absence of the threshold $h = J$ where the probabilities p and q change their forms, and subsequently a fully smooth transition between $h < J$ and $h > J$ regimes. Figure 9 presents a comparison between single-update (solid line) and spin -thermalization approaches (dotted line) for $h < J$ supported with numerical simulations. The plot proves that although there is a difference

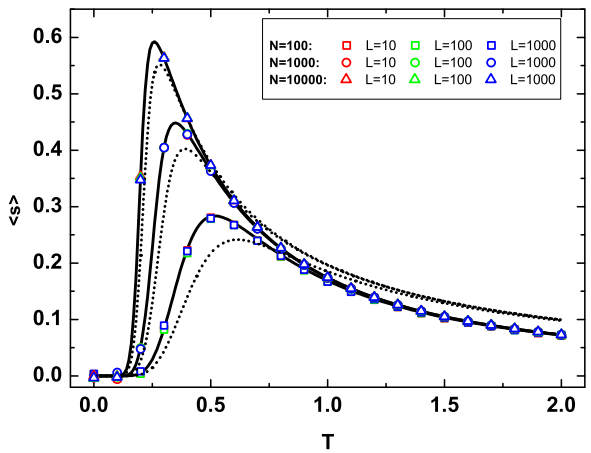

FIG. 9. (Color online) Chain magnetization $\langle s \rangle$ versus temperature T for single-step update [dotted line, given by Eq. (4)] and single-spin thermalization [solid line, given by Eq. (18)] with $h = 0.1$ and $J = 1$. Points represent numerical simulations for chain of length N with L steps of update procedure averaged over $M = 10^5$ realizations.

in the crossover temperature as well as in the peak height, the character of the curve is kept the same.

VIII. REAL DATA

The developed method can be compared with the real data on emotional interactions in online media: *BBC Forum* [30,31] and *Digg* [32,33]. Those data sets (see Table I for their properties) contain several messages whose emotional content had first been in small part annotated by humans and then those results served as an input to an automatic sentiment detection classifier software [34]. Owing to the supervised, machine-learning approach [35] it was then possible to detect the level of emotional valence [27] (negative $e_i = -1$, neutral $e_i = 0$, or positive $e_i = +1$) for each comment with a reasonable accuracy rate [22,33].

In order to obtain the values of h and T we proceed as follows: (i) we choose discussions (threads) possessing only negative and positive comments and we put them in a chronological order (see values N_d^{+-} and N_c^{+-} in Table I); (ii) for each set of threads we calculate a fraction of negative and positive comments [respectively, $p(-)$ and $p(+)$] and conditional probabilities $p(e|e)$ that two consecutive messages have the same valence, defined as $p(e|e) = p(ee)/p(e)$, where $p(ee)$ is the joint probability of the pair ee measured as the total number of occurrences of the two consecutive messages with the same valence e divided by the number of all appearing pairs; (iii) we aggregate all threads of the same length N by calculating average values of $p(-|-)$ and $p(+|+)$; (iv) finally, we identify $p(-|-)$ and $p(+|+)$ with the probabilities $\Pr(-|-)$ and $\Pr(+|+)$ given by Eq. (3). Then, using Eq. (3) one is able to get the values of h and T. When $h < -1$ then

$$\begin{cases} T = \dfrac{4}{\ln \frac{\Pr(+|+)}{1-\Pr(-|-)}} \\ h = \dfrac{\ln\{4\Pr(+|+)[1-\Pr(-|-)]\}}{\ln \frac{\Pr(+|+)}{1-\Pr(-|-)}} \end{cases}, \tag{20}$$

when $|h| \leqslant 1$ then

$$\begin{cases} T = -\dfrac{4}{\ln 4[1-\Pr(+|+)][1-\Pr(-|-)]} \\ h = \dfrac{\ln \frac{1-\Pr(+|+)}{1-\Pr(-|-)}}{\ln 4[1-\Pr(+|+)][1-\Pr(-|-)]} \end{cases}, \tag{21}$$

when $h > 1$ then

$$\begin{cases} T = \dfrac{4}{\ln \frac{\Pr(-|-)}{1-\Pr(+|+)}} \\ h = -\dfrac{\ln\{4\Pr(-|-)[1-\Pr(+|+)]\}}{\ln \frac{\Pr(-|-)}{1-\Pr(+|+)}} \end{cases}. \tag{22}$$

It is important to notice here that because of the above given conditions ($h < -1$, $|h| \leqslant 1$, and $h > 1$) as well as the overall assumption $T \geqslant 0$, the conditional probabilities $\Pr(-|-)$ and $\Pr(+|+)$ are not independent and they are bound with the condition

$$\Pr(-|-) \geqslant 1 - \Pr(+|+). \tag{23}$$

TABLE I. Properties of two real-world datasets *BBC Forum* and *Digg* used as validation cases for the model: N_d, N_c are the total number of discussions and comments in the original datasets; $p(-)$, $p(0)$, and $p(+)$ are, respectively, probabilities that a randomly chosen comment is negative, neutral, or positive (i.e., the fractions of negative, neutral, and positive comments); $\langle e\rangle = p(+) - p(-)$ stands for the average emotional value of the dataset; $p(-|-)$, $p(0|0)$, $p(+|+)$ are conditional probabilities of negative (respectively, neutral and positive) comment followed by a comment of the same valence; N_d^{+-} is the number of discussions consisting only of negative and positive and N_c^{+-} gives the summed number comments in such discussions; M stands for the number of data points seen in Fig. 10 and M_v is number of data points fulfilling the condition Eq. (23).

Data set	N_d	N_c	$p(-)$	$p(0)$	$p(+)$	$\langle e\rangle$	$p(-\|-)$	$p(0\|0)$	$p(+\|+)$	N_d^{+-}	N_c^{+-}	M	M_v
BBC Forum	97 946	2 747 781	0.65	0.16	0.19	−0.44	0.69	0.20	0.27	3373	53 664	49	15
Digg	129 998	1 646 153	0.48	0.21	0.31	−0.16	0.56	0.27	0.37	742	10 123	28	10

Figure 10 presents conditional probability $\Pr(+|+)$ versus $\Pr(-|-)$ for BBC Forum and Digg data (left panel) together with some examples of discussions in those media (right panel). Around 70% of the data lays in the area prohibited by relation Eq. (23), which could suggest that the simplifications assumed in our model regarding the short-range memory of users could be inappropriate for this system. On the other hand, it is essential to notice that in the real-data analysis the probabilities of drawing the spins before the update procedure are unknown as they are *a priori* values. The other difficulty comes from the fact that the data are aggregated over the discussion size by calculating the average values of probabilities. Nonetheless, the presented examples of discussions show that for $|h| < 1$ we can observe similar structures as postulated in Fig. 6(a) [case (d) on the right panel of Fig. 10]. Moreover, it seems that the majority of the discussions are located in the area of high temperature and high negative field, which coincides with the average emotional value of the data (see Table I) and suggests both tendency to follow the overall sentiment in the medium as well as a significant level of uncertainty about one's emotion.

IX. CONCLUSIONS

In summary, we have demonstrated that the finite system size and initial conditions can lead to the emergence of a nonmonotonous dependence of the mean magnetization on the system's temperature in a growing one-dimensional Ising model with quenched spins. The effect exists only for magnetic fields smaller than the value of the spin coupling constant and the crossover temperature decays to zero very slowly with the system size. Using Markov chain theory we have developed an analytical approach to this phenomenon that well fits numerical simulations. The effect can be understood as a competition between thermal fluctuations and the influence of the initial condition that fixes orientation of spins in the first cluster. The crossover temperature can be explained as the point where the initial ordered cluster (domain) is no longer dominant thanks to thermal fluctuations, yet the temperature did not lower much the average magnetization toward zero. The effect exists also when spins are not quenched but fully thermalized after the attachment to the chain. The absence of the effect for the higher magnetic field is the result of a transition from a bistable to a monostable energy landscape of a pair of neighboring spins.

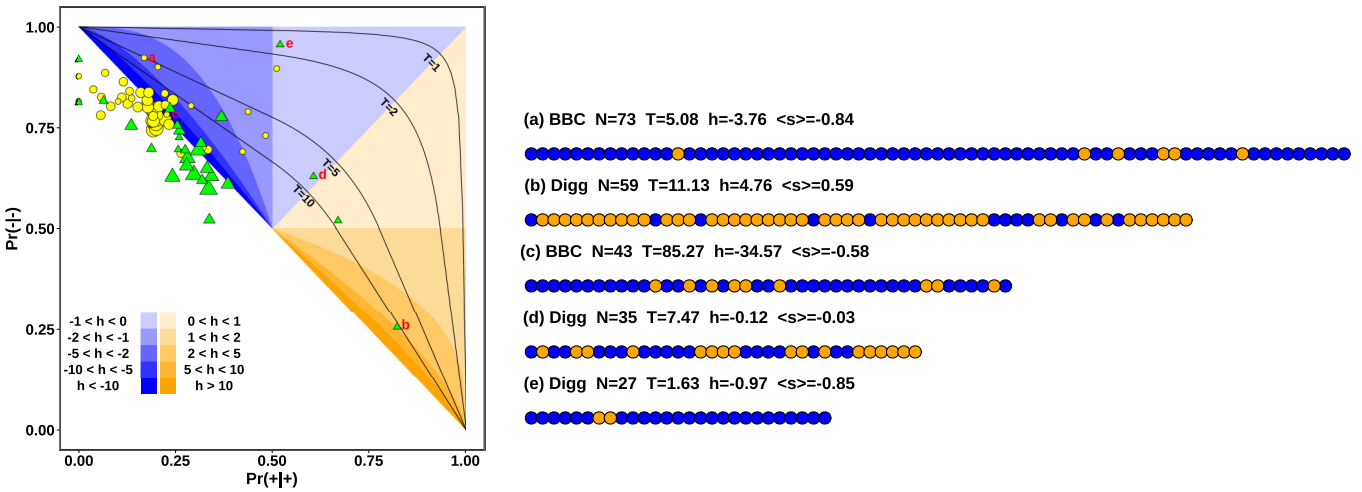

FIG. 10. (Color online) (left panel) Conditional probability $\Pr(-|-)$ versus conditional probability $\Pr(+|+)$ for *BBC Forum* (circles) and *Digg* (triangles) data; the size of the symbol is proportional to the logarithm of the number of aggregated discussions. The borders of the shaded regions represent isolines of constant magnetic field h while the solid black lines are isotherms—in both cases the values were obtained from Eqs. (20)–(22). The white region represents the area where there are no solutions provided by Eqs. (20)–(22) if assumed that $T \geqslant 0$. (right panel) Examples of actual chronologically ordered discussions from *BBC Forum* and *Digg* data; orange (blue) discs symbolize positive (negative) comments and the letters (a)–(e) can be used to localize the discussion in the left panel.

We think that, although directly inspired by the clustering phenomena observed in the online emotional discussions [22,23], the model can open an interesting playground for all systems where initial conditions and finite-size effects are relevant.

ACKNOWLEDGMENTS

This work was supported by a European Union grant by the 7th Framework Programme, Theme 3: Science of Complex Systems for Socially Intelligent ICT. It is part of the CyberEMOTIONS (Collective Emotions in Cyberspace) project (Contract No. 231323). We also acknowledge support from Polish Ministry of Science Grant No. 1029/7.PR UE/2009/7. This work has also been supported by the European Union in the framework of European Social Fund through the Warsaw University of Technology Development Programme, realized by the Center for Advanced Studies.

APPENDIX: DERIVATION OF THE MEAN MAGNETIZATION

Let us calculate the probability that a spin-up follows another spin-up. We assume the presence of external field $h \geqslant 0$. First, we set $s_0 = +1$. Then, with equal probabilities $\Pr(s_1 \pm 1) = 1/2$, spin in the next node is chosen to be up or down. Next, we calculate the change of function $\mathcal{E}$, given by

$$\Delta\mathcal{E} = \mathcal{E}_1' - \mathcal{E}_1 = -(Js_0 + h)(s_1' - s_1), \tag{A1}$$

which follows

(1) if $s_1 = +1$ and $s_1' = -1$, then $\Delta\mathcal{E} = 2(h + J) > 0$, so the change is accepted with probability equal to $e^{-\widetilde{\beta}(h+J)}$ and not accepted with probability equal to $1 - e^{-\widetilde{\beta}(h+J)}$, where $\widetilde{\beta} = 2/(k_B T)$,

(2) if $s_1 = -1$ and $s_1' = +1$, then $\Delta\mathcal{E} = -2(h + J) < 0$, so the change is always accepted.

As a consequence, the probability p_{++} of a spin-up following another spin-up is equal to $p_{++} = \frac{1}{2}(1 - e^{-\widetilde{\beta}(h+J)}) + \frac{1}{2} \times 1 = 1 - \frac{1}{2}e^{-\widetilde{\beta}(h+J)}$. Then, for $h \geqslant 0$ we have

$$\begin{cases} p_{++} = \Pr(+|+) = 1 - \frac{1}{2}e^{-\widetilde{\beta}(h+J)} \\ p_{+-} = \Pr(-|+) = 1 - p_{++} \end{cases}. \tag{A2}$$

Now let us calculate the probability that a spin-down follows another spin-down. Contrary to the previous case we set $s_0 = -1$ and then, with equal probabilities $\Pr(s_1 \pm 1) = 1/2$, spin in the next node is chosen to be up or down. Next, we calculate the change of function $\mathcal{E}$

(1) if $s_1 = -1$ and $s_1' = +1$ then $\Delta\mathcal{E} = -2(h - J)$,

(2) if $s_1 = +1$ and $s_1' = -1$ then $\Delta\mathcal{E} = 2(h - J)$.

Here, the issue of the spin change being accepted or not depends on the value of external field:

(i) if $0 \leqslant h < J$, then

(1) for $s_1 = -1$ and $s_1' = +1$ we have $\Delta\mathcal{E} > 0$, so the change is accepted with probability $e^{\widetilde{\beta}(h-J)}$ and not accepted with probability equal to $1 - e^{\widetilde{\beta}(h-J)}$

(2) for $s_1 = +1$ and $s_1' = -1$ we have $\Delta\mathcal{E} < 0$, so the change is always accepted,

(ii) if $h \geqslant J$, then the character $-1 \to +1$ and $+1 \to -1$ changes since signs of energy difference $\Delta\mathcal{E}$ rearrange

(1) for $s_1 = -1$ and $s_1' = +1$, we have $\Delta\mathcal{E} < 0$, so the change is always accepted,

(2) for $s_1 = +1$ and $s_1' = -1$, we have $\Delta\mathcal{E} > 0$, so the change is accepted with probability $e^{-\widetilde{\beta}(h-J)}$ and not accepted with probability equal to $1 - e^{-\widetilde{\beta}(h-J)}$.

As a consequence, the probability p_{--} of a spin-down following another spin-down is equal to $p_{--} = \frac{1}{2}(1 - e^{\widetilde{\beta}(h-J)}) + \frac{1}{2} \times 1$ for $0 \leqslant h < J$ and $p_{--} = \frac{1}{2} \times 0 + \frac{1}{2} \times e^{-\widetilde{\beta}(h-J)}$ for $h \geqslant J$. Thus, we have

$$\begin{cases} p_{--} = \Pr(-|-) = 1 - \frac{1}{2}e^{\widetilde{\beta}(h-J)} \\ p_{-+} = \Pr(+|-) = 1 - p_{--} \end{cases}, \tag{A3}$$

for $0 \leqslant h < J$, and

$$\begin{cases} p_{--} = \Pr(-|-) = \frac{1}{2}e^{-\widetilde{\beta}(h-J)} \\ p_{-+} = \Pr(+|-) = 1 - p_{--} \end{cases}, \tag{A4}$$

for $h \geqslant J$.

For simplicity of the further calculations we use the following notation: the probability to stay in $+1$ state is $p_{++} = p$; the probability to move from state $+1$ to state -1 is $p_{+-} = 1 - p$. Similarly, we denote the probability to stay in -1 as $p_{--} = q$ and the probability to move from state -1 to $+1$ is $p_{-+} = 1 - q$. In effect we obtain the transition matrix $\mathbf{P}$ given by Eq. (1), which defines probabilities evolution of both states $\Pr(s_n = \pm 1)$,

$$\mathbf{s}_{n+1} = \mathbf{s}_n \mathbf{P}, \tag{A5}$$

where $\mathbf{s}_n = [\Pr(s_n = +1) \quad \Pr(s_n = -1)]$. Thus, the evolution of $\mathbf{s}_n$ is in fact an equivalent of a two-state Markov chain [29] governed by the transition matrix $\mathbf{P}$. Appropriate elements of the nth power of matrix $\mathbf{P}$ give the probabilities that the chain that started with a specific spin has a certain spin in its nth node [e.g., $(\mathbf{P}^n)_{11}$ is the probability that after starting $s_0 = +1$ the spin in the nth node will also be also $s_n = +1$]. A short algebra leads to

$$\mathbf{P}^n = \begin{Bmatrix} \frac{q-1+(p-1)(q+p-1)^n}{q+p-2} & \frac{(p-1)[1-(q+p-1)^n]}{q+p-2} \\ \frac{(q-1)[1-(q+p-1)^n]}{q+p-2} & \frac{p-1+(q-1)(q+p-1)^n}{q+p-2} \end{Bmatrix}. \tag{A6}$$

Subtracting the second column from the first one in matrix $\mathbf{P}^n$ leads to equations describing the average spin values $\langle s^n \rangle_\pm$ in the nth node, assuming that the first node contained a specific spin orientation ($s_0 = +1$ or $e_0 = -1$):

$$(\mathbf{P}^n)_{11} - (\mathbf{P}^n)_{12} = \langle s_n \rangle_+ = \frac{p - q - 2(p-1)(p+q-1)^n}{2 - p - q} \tag{A7}$$

$$(\mathbf{P}^n)_{21} - (\mathbf{P}^n)_{22} = \langle s_n \rangle_- = \frac{p - q + 2(q-1)(p+q-1)^n}{2 - p - q}. \tag{A8}$$

Calculating the average value of $\langle s_n \rangle_+$ and $\langle s_n \rangle_-$ leads to the average spin in the nth node:

$$\langle s_n \rangle = \frac{\langle s_n \rangle_+ + \langle s_n \rangle_-}{2} = \frac{(p-q)[1-(p+q-1)^n]}{2 - p - q}. \tag{A9}$$

The plots of $\langle s_n \rangle_+$, $\langle s_n \rangle_-$, and $\langle s_n \rangle$ versus n for selected values of the external field h and temperature T are shown in Fig. 11.

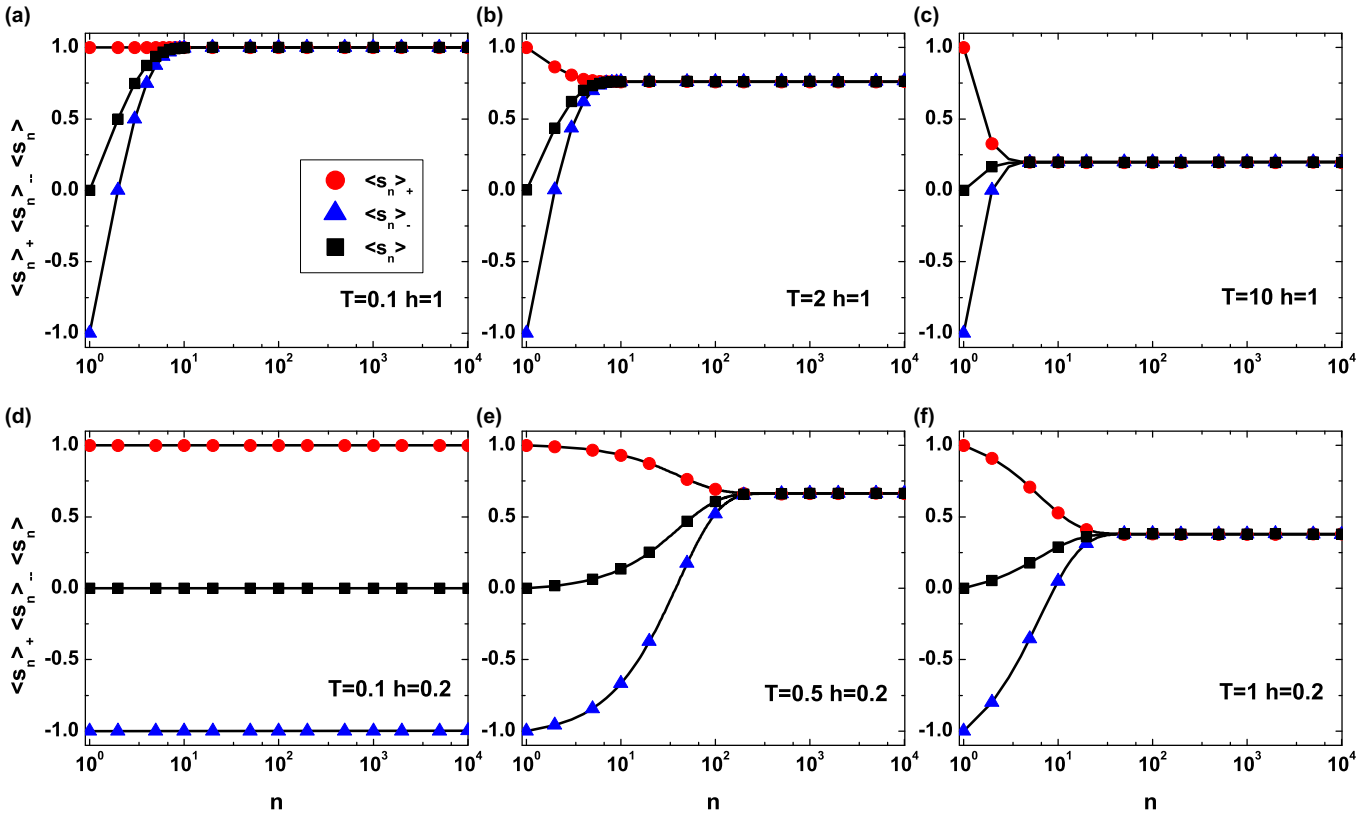

FIG. 11. (Color online) Average spin $\langle s_n \rangle$ in the nth node and average spin if the nth node starting from an up-spin $\langle s_n \rangle_+$ and down-spin $\langle s_n \rangle_-$ for selected parameters h and T. Symbols are numerical simulations and solid lines come from Eqs. (A7), (A8), and (A9).

One can easily observe the convergence of $\langle s_n \rangle$ to a constant value for a sufficiently large value of n. In fact, as $p+q-1<1$, we have $\lim_{n\to\infty}\langle s_n \rangle = (q-p)/(p+q-2)$.

Finally, performing the sum of $\langle s_n \rangle$ over all nodes in the chain gives the average spin:

$$\langle s \rangle = \frac{1}{N}\sum_{n=1}^{N}\langle s_n \rangle. \tag{A10}$$

Similar calculations can be performed for ranges $h \in (-\infty; -J]$ and $h \in (-J; 0]$. The symmetry of the problem results in swapping all the indices "+" to "−" and likewise as well as putting "−" sign in front of h in Eqs. (A2)–(A4). As an outcome we obtain a rotated matrix $\mathbf{P}$ that leads again to Eq. (A9). In effect, by applying exact values of the probabilities p and q given by Eqs. (A2)–(A4), we obtain the average spin for $|h| < J$ as Eq. (4) and for $|h| \geqslant J$ as Eq. (5).

[1] E. Ising, Z. Phys. **31**, 253 (1925).
[2] D. Ruelle, Commun. Math. Phys. **9**, 267 (1968).
[3] F. J. Dyson, Commun. Math. Phys. **12**, 91 (1969).
[4] J. Fröhlich and T. Spencer, Commun. Math. Phys. **84**, 87 (1982).
[5] D. J. Thouless, Phys. Rev. **187**, 732 (1969).
[6] G. Grinstein and D. Mukamel, Phys. Rev. B **27**, 4503 (1983).
[7] P. Bak and R. Bruinsma, Phys. Rev. Lett. **49**, 249 (1982).
[8] S. I. Denisov and P. Hänggi, Phys. Rev. E **71**, 046137 (2005).
[9] M. B. Yilmaz and F. M. Zimmermann, Phys. Rev. E **71**, 026127 (2005).
[10] J. K. Percus, J. Stat. Phys. **16**, 299 (1977).
[11] G. De Chiara, L. Lepori, M. Lewenstein, and A. Sanpera, Phys. Rev. Lett. **109**, 237208 (2012).
[12] T. Koffel, M. Lewenstein, and L. Tagliacozzo, Phys. Rev. Lett. **109**, 267203 (2012).
[13] K. Huang, *Statistical Mechanics* (Wiley & Sons, New York, 1987).
[14] H. W. Huang, Phys. Rev. B **12**, 216 (1975).
[15] K. G. Chakraborty, Phys. Rev. B **20**, 2924 (1979).
[16] M. L. Mansfield, Phys. Rev. E **66**, 016101 (2002).
[17] K. Sznajd-Weron and J. Sznajd, Int. J. Mod. Phys. C **11**, 1157 (2000).
[18] Z. Liu, J. Luo, and Ch. Shao, Phys. Rev. E **64**, 046134 (2001).
[19] P. Kondratiuk, G. Siudem, and J. A. Hołyst, Phys. Rev. E **85**, 066126 (2012).
[20] J. Sienkiewicz and J. A. Hołyst, Phys. Rev. E **80**, 036103 (2009).
[21] J. Sienkiewicz, G. Siudem, and J. A. Hołyst, Phys. Rev. E **82**, 057101 (2010).
[22] A. Chmiel, J. Sienkiewicz, M. Thelwall, G. Paltoglou, K. Buckley, A. Kappas, and J. A. Hołyst, PLoS ONE **6**, e22207 (2011).

[23] A. Chmiel and J. A. Hołyst, Phys. Rev. E **87**, 022808 (2013).
[24] F. Schweitzer and D. Garcia, Eur. Phys. J. B **77**, 533 (2010).
[25] D. Garcia, A. Garas, and F. Schweitzer, EPJ Data Sci. **1**, 3 (2012).
[26] M. Mitrović and B. Tadić, Physica A **391**, 5264 (2012).
[27] L. A. Feldman, J. Personal. Soc. Psychol. **69**, 153 (1995).
[28] N. Metropolis, A. W. Rosenbluth, M. N. Rosenbluth, A. H. Teller, and E. Teller, J. Chem. Phys. **21**, 1087 (1953).
[29] J. R. Norris, *Markov Chains* (Cambridge University Press, New York, 1997).
[30] http://www.bbc.co.uk/dna/mbreligion, http://www.bbc.co.uk/dna/mbfivelive.
[31] A. Chmiel, P. Sobkowicz, J. Sienkiewicz, G. Paltoglou, K. Buckley, M. Thelwall, and J. A. Hołyst, Physica A **390**, 2936 (2011).
[32] http://www.digg.com.
[33] P. Pohorecki, J. Sienkiewicz, M. Mitrović, G. Paltoglou, and J. Hołyst, Acta Phys. Pol. A **123**, 604 (2013).
[34] M. Mitrović, G. Paltoglou, and B. Tadić, Eur. Phys. J. B **77**, 597 (2010).
[35] F. Sebastiani, ACM Comput. Surv. **34**, 1 (2002).